Novel thermal conductivity enhancing containers for performance enhancement of solar photovoltaics system integrated with phase change material

Sourav Khanna[a,*,1], Preeti Singh[b,1], Vijay Mudgal[c,d], Sanjeev Newar[b], Vashi Sharma[b], Victor Becerra[a], K. S. Reddy[e], Tapas K. Mallick[f]

[a] School of Energy and Electronic Engineering, Faculty of Technology, University of Portsmouth, Portsmouth PO1 3DJ, UK
[b] Indian Institute of Technology Kanpur, Uttar Pradesh 208016, India
[c] University Centre for Research and Development, Chandigarh University, Mohali 140 413, Punjab, India
[d] Electrical Engineering Chandigarh University, Mohali 140 413, Punjab, India
[e] Department of Mechanical Engineering, IIT Madras, Tamil Nadu 600036, India
[f] Environment and Sustainability Institute, University of Exeter, Penryn TR10 9FE, UK

Abstract: Phase change material (PCM) has capability to increase the power production of solar photovoltaics (PV) by effective temperature regulation. In this work, Thermal Conductivity Enhancing Containers (TCEC) are proposed. They allow the PCM to extract the heat from all sides of the containers instead of only front which improves the thermal conductivity of the PCM containers and increases the PV electrical efficiency. PCM was filled inside the TCECs and pasted at the back of the PV. Systems with and without PCM, with and without TCEC and systems with different tilt angles have been investigated. The melting of PCM, rate of thermal energy storage, charging efficiency and enhancement in PV performance are analyzed. The behavior of the systems is analyzed for the climates of Portsmouth, UK and Chennai, India. It is seen that the average charging efficiency of PCM can be increased from 49% to 62% using proposed TCEC. Moreover, the average rate of thermal energy storage can be increased from 249W/m^2 of aperture to 302W/m^2 and the PV electrical efficiency can be increased from 17.6% to 19.2% using TCEC-PCM. It is also seen that as the inclination of PCM container decreases from 45° to 0°, the charging efficiency decreases by 32%.

Keywords: charging efficiency; energy storage; solar; photovoltaics; phase change material

[1] First Authors

* Corresponding author

Email: sourav.khanna@port.ac.uk; sourav.khanna1@gmail.com

1. Introduction

Solar energy is a renewable, abundant and clean source from which electricity and thermal output can be derived. Electricity can be produced directly from solar energy using solar photovoltaics (PV) that use semiconductor material [1]. However, the temperature of the material raises in the exposure of sun which reduces the power production efficiency [2]. To avoid the reduction in efficiency, PV cooling is required [3]. There are active cooling methods to increase the performance of PV but they increase the operating and maintenance (O&M) cost of the PV system too [4]. To avoid the additional operating cost, passive cooling methods have also been explored. Phase change material (PCM) based passive cooling has capability to increase the power production of PV by effective temperature regulation as PCM can absorb huge amount of energy during melting/ charging [5]. It has also been reported that the PV efficiency decreases every year due to degradation [6]. However, PCM has capability to increase the lifetime of the PV panel by 30% by regulating the operating temperature of the PV [7]. Chowdhury et al. [8] presented a review of PV cooling using PCM and listed down the desirable properties of a good PCM such as high thermal conductivity and high latent heat capacity.

1.1. Integration of PV with Paraffin wax

Huang et al. [9, 10] used paraffin wax (RT 25) as PCM and attached it behind a PV. They reported that the paraffin wax can cool the PV effectively and maintain it below 38°C for 180 min. In another study, they used RT32 paraffin wax for PCM based cooling and the effect of solar irradiance was studied. It was reported that the duration of cooling shortened from 110 min to 80 min with increase in irradiance from 800 to 1000W/m^2. However, it must be noted that they used mimicked PV. Khanna et al. [11] used a real PV and RT25HC paraffin wax for a numerical study and found that the cooling duration can be extended from 3.8h to 6.4h by increasing the depth of the PCM container from 3cm to 5cm. Elarga et al. [12] attached

the PCM with PV in a double-skin facade configuration and found that it reduced monthly cooling demand by 20-30% and enhanced the electrical efficiency of the system by 5-8%. Singh et al. [13] carried out a sensitivity analysis to analyze the effect of different parameters on the working of PCM. It was reported that the PV cooling strongly depends on the seasons and climates. It was observed that the PCM is more productive in hot and less windy climates and less productive for cold climates [14]. Sarwar et al. [15] studied the effect of PCM's thermal conductivity, melting point, heat of fusion and ambient temperature and found that the increase in the ambient temperature from 25°C to 50°C can decrease the PV electrical output by 10% and increase in thermal conductivity can increase the PV electrical output by 3.5%.

1.2. Integration of PV with various types of PCMs

Paraffin wax is the most investigated PCM for the PV cooling application [16] due to its availability in a wide range of melting points. However, researchers have also investigated other types of PCMs. Hasan et al. [17] used capric–palmitic acid (PCM_1) and calcium chloride hexahydrate (PCM_2) and attached at the back of the polycrystalline silicon PV panel. It was found that the PCM_1 can increase the PV power production by 4.4% on an average for hot climate and 1% for cold climate whereas PCM_2 can increase the PV power production by 7.7% for hot climate and 1.8% for cold climate. Karthick et al. [18] used inorganic glauber salt as PCM and attached at the back of a building integrated PV and reported a maximum reduction of 8°C in the PV temperature, an increase of 10% in the electrical efficiency and a mitigation of 1.74 tCO_2e over the lifetime of the panel. In another study, Karthick et al. [19] used inorganic glauber salt for the cooling of a semitransparent PV and found a reduction of 12°C in the peak PV temperature and an increase of 3kWh in the annual electricity generation. Thaib et al. [20] used beeswax as PCM and reported an increase of 15% in the

electrical efficiency. Abdollahi and Rahimi [21] used a mixture of coconut oil and sunflower oil as PCM and reported a reduction of 20°C in PV temperature.

1.3. Enhancement of rate of heat transfer

One common limitation of all the PCMs is their very low thermal conductivity (around 1W/m-K) which restricts its potential for PV cooling purposes. Thus, the additional investment in the form of PCM can be higher than that of the savings in certain cases [22]. However, the increase in the thermal conductivity and the optimization of PCM quantity can make the system profitable. Thus, researchers have investigated the optimization of the thermal conductivity of the PCM [23]. To improve the performance of PCM, researchers have also inspected novel synthesized PCMs using nanoparticles such as Al_2O_3, CuO, MgO [24], SiC [25] and SiO_2. Zarma et al. [26] reported that the addition of Al_2O_3 increased the thermal conductivity of PCM significantly as compared to CuO and SiO_2. It has also been noticed that the rise in the nanoparticle loading ratio increased the cooling effect of PCM. Sharma et al. [27] reported that the addition of CuO nano particles increased the thermal conductivity of PCM (RT42) by 0.35%. The results also showed that the addition of nanoparticles improved the PV temperature reduction from 9.6°C to 11.2°C. Manigandan and Kumar [28] reported that the addition of PCM and CuO nano fluid increased the system electric output by 15%. Salem et al. [29] observed that 1% nanoparticle (Al_2O_3) concentration with 24% PCM and 75% water increased the electrical efficiency of PV panel by 22.7% whereas only-PCM case increased the electrical efficiency by 15.7% compared to reference PV panel. Nada and Nagar [30] observed that the integration of PCM with PV increased the average efficiency of the PV panel by 7.1%. It was also observed that the addition of 2% nanoparticle (Al_2O_3) to PCM further enhanced the efficiency of the panel by 7.1%. Researchers have also explored the use of expanded-graphite [31], Cu-foam, fins [32] and metal-matrix [33] to enhance the performance of PCM for PV cooling purpose. Abdelrahman

et al. [34] experimentally evaluated the performance of the PV panel integrated with fins, PCM and nano-particles. It was reported that a reduction of 34.5°C in the PV temperature can be achieved. Wongwuttanasatian et al. [35] observed that the PV integration with PCM in finned box reduced additional 6.1°C of PV panel temperature and increased 5.3% of panel efficiency compared to PV panel with PCM without fins. The literature review on the enhancement of rate of heat transfer is also presented in Table 1.

1.4. Research Gap

Out of many research gaps, a few are given as follows:

(i) It has been found that the PCM does not solidify homogenously during discharging phase. Thus, the contact of the solid PCM with the walls of the container is not perfect which can reduce the rate of heat transfer. Thus, it should be incorporated in the modeling.

(ii) It must also be mentioned that the contact of the PV rear with the aluminium container is not perfect in reality which can reduce the rate of heat transfer too. Thus, the contact resistances should also be incorporated in the modelling.

(iii) It is also reported that the thermal conductivity of the phase change material is low which restricts its potential in the application of PV cooling. The low thermal conductivity will reduce its charging efficiency. Thus, efforts are required to enhance the charging efficiency of the PCM which will enhance the PV performance too.

1.5. Proposed Methodology

In the present study, thermal conductivity enhancing containers (TCEC) are proposed. The TCECs have been filled with PCM and integrated at the rear of the PV. In this system, the heat from the PV easily travels to the back of the containers. Thus, the PCM is able to extract the heat from all sides of the containers instead of only front. It increases the thermal conductivity of the overall PCM container which enhances the charging efficiency of the

PCM. In this study, the melting of PCM, charging efficiency, rate of heat storage and enhancement in PV performance have been analyzed.

Table 1: Literature on the enhancement of rate of heat transfer

Reference	**Improvement**	**Technique Used**
Sharma et al. [27]	Increment in thermal conductivity of PCM by 0.35%	Addition of CuO nano particles
Manigandan and Kumar [28]	Improvement in electric output by 15%	Addition of PCM and CuO nano fluid
Salem et al. [29]	Improvement in electrical efficiency of PV panel by 22.7%	Addition of 1% Al_2O_3, 24% PCM and 75% water.
Nada and Nagar [30]	Improvement in electrical efficiency of PV panel by 14.2%	Addition of 2% nanoparticle (Al_2O_3) with PCM
Abdelrahman et al. [34]	Reduction in PV temperature by 34.5°C	Addition of nanoparticles (Al_2O_3) with PCM and fins
Wongwuttanasatian et al. [35]	Reduction in PV temperature by 6.1°C	Addition of fins

2. Modelling

Seven PV systems are investigated as shown in Fig. 1. The PV panels in all the systems are made up of mono-si based material. 1st system is the uncooled PV panel. The dimensions of the panel are 1020 mm x 980 mm with a power rating of 200 Wp, electrical efficiency (at

STC) of 20%, open circuit voltage of 32.9 V, short circuit current of 8.21 A, voltage corresponding to maximum power is 26.3 V and current corresponding to maximum power is 7.61 A. 2nd system is the PV-PCM system (Fig. 1b) in which the PCM container is attached at the back of the PV keeping tilt at 45°. For PCM, paraffin wax based material is considered having melting point around 291K. The properties of the PCM and measurements of the container are given in Appendix A. 3rd system is the PV-TCEC-PCM system in which both PCM and TCECs are attached at the back of the PV keeping tilt at 45°as shown in Fig. 1c. TCECs are made up of aluminium and the measurements are given in Appendix A. 4th system is a horizontal PVPCM system (tilt 0°). 5th, 6th and 7th systems are same as that of 4th but with different tilt angles 15°, 30° and 45° respectively.

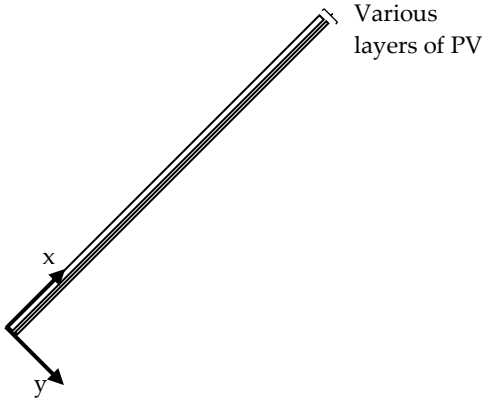

(**a**) 1st system

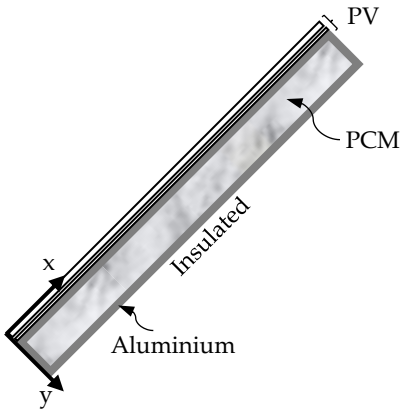

(**b**) 2nd system

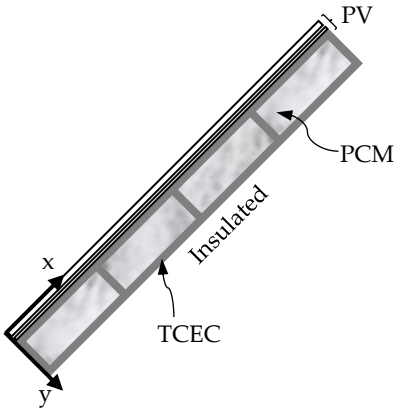

(**c**) 3rd system

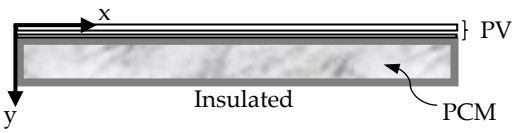

(**d**) 4th system

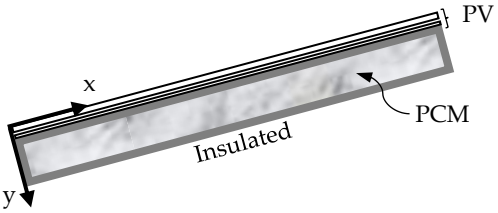

(**e**) 5th system

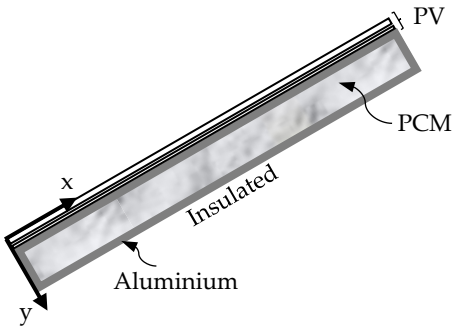

(**f**) 6th system

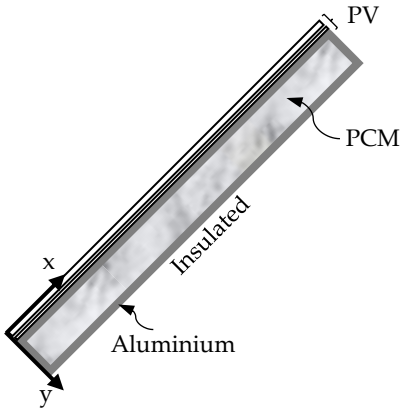

(**g**) 7th system

Figure 1. Studied systems: (**a**) 1st system: Uncooled PV; (**b**) 2nd system: PV-PCM system with 45° tilt; **(c)** 3rd system: PV-TCEC-PCM system with 45° tilt; **(d)** 4th system: PV-PCM system with 0° tilt; **(e)** 5th system: PV-PCM system with 15° tilt; **(f)** 6th system: PV-PCM system with 30° tilt ; **(g)** 7th system: PV-PCM system with 45° tilt.

In order to analyze the melting of PCM, rate of energy storage, charging efficiency and the power production efficiency, the following equations are used.

2.1. Solid Region

The rate of change of temperature with time ($\partial T_j/\partial t$) for the j^{th} solid layer of the systems can be calculated using Eq. (1) in terms of heat generation (G_j), density (ρ_j), specific heat ($C_{p,j}$) and thermal conductivity (k_j). The left hand side (LHS) of the equation is the rate of change of energy. First term on the right hand side (RHS) is the rate of heat generation and second term on RHS corresponds to the rate of heat flowing due to conduction.

$$\rho_j C_{p,j} \frac{\partial T_j}{\partial t} = G_j + k_j \left(\frac{\partial^2 T_j}{\partial x^2} + \frac{\partial^2 T_j}{\partial y^2} \right) \quad (1)$$

The heat loss from the front surface of the photovoltaic module (i.e. glass) can be calculated using Eq. (2). The LHS of the equation gives the rate of energy going out from the front of the PV. First term on the RHS is the heat losses due to convection in terms of heat transfer coefficient (h), glass temperature (T_g) and ambient temperature (T_a). Second term is the heat losses due to radiation in terms of Stefan-Boltzmann constant (σ), emissivity (ε), glass temperature and surroundings (sky) temperature (T_s).

$$k_g \frac{\partial T_g}{\partial y} = h\left[T_g - T_a\right] + \sigma\varepsilon\left[T_g^4 - T_s^4\right] \ at\ PV\ front \quad (2)$$

The heat loss from the sides of each j^{th} layer can be neglected due to negligible thickness as compared to other dimensions (length and width). The LHS of the equation gives the rate of energy going out from the sides.

$$-k_j \frac{\partial T_j}{\partial x} = 0 \ at\ sides \quad (3)$$

The heat from the back surface of the photovoltaic module (tedlar) will be flown towards the aluminium container and this equality can be given by Eq. (4). The LHS of the equation gives the rate of energy going out from the back of the tedlar in terms of thermal conductivity (k_t) and temperature (T_t). The RHS of the equation gives the rate of energy entering the front of the aluminium container in terms of thermal conductivity (k_{al}) and temperature (T_{al}).

$$-k_t \frac{\partial T_t}{\partial y} = -k_{al} \frac{\partial T_{al}}{\partial y} at\ PV\ back \tag{4}$$

The rate of heat leaving from the bottom of the uncooled system (1st system) is equal to the heat losses due to the convection and radiation.

$$-k_t \frac{\partial T_t}{\partial y} = h[T_t - T_a] + \sigma\varepsilon[T_t^4 - T_s^4] \qquad for\ uncooled\ system \tag{5}$$

The rate of heat leaving from the bottom of the cooled systems is equal to nil because of the adiabatic boundaries.

$$-k_{al} \frac{\partial T_b}{\partial y} = 0 \tag{6}$$

Before sunshine, the temperature of each j^{th} layer is same as that of the ambient. Thus,

$$T_j = T_a\ before\ sunshine \tag{7}$$

2.2 Phase Change Material

The rate of change of temperature of PCM with time ($\partial T_P/\partial t$) can be calculated using Eq. (8) in terms of density (ρ_P), specific heat ($C_{p,P}$), thermal conductivity (k_P), temperature (T_P), and velocity of PCM in x direction (u_x) and in y direction (u_y). The LHS of the equation is the rate of change of energy. The RHS of the equation is the rate of heat flowing due to conduction and convection.

$$\rho_P C_{p,P} \frac{\partial T_P}{\partial t} = \nabla.(k_P \nabla T_P) - \frac{\partial}{\partial x}\left(\rho_P C_{p,P} u_x T_P\right) - \frac{\partial}{\partial y}\left(\rho_P C_{p,P} u_y T_P\right) \quad (8)$$

The latent heat capacity of PCM (L_P) is incorporated in the form of specific heat ($C_{p,P}$) in the phase change zone ($T_s < T_P < T_l$). T_s is the temperature below which PCM is solid and T_l is the temperature above which it is liquid. Specific heat capacity is modelled in Eq. (9) in terms of specific heat capacity in solid phase ($C_{p,P,s}$), specific heat capacity in liquid phase ($C_{p,P,l}$), latent heat capacity, liquid faction (l) [36] and Dirac delta function (D) [36].

$$C_{p,P}(T_P) = \begin{cases} C_{p,P,s} & if\ T_P \le T_s \\ C_{p,P,s} + \left(C_{p,P,l} - C_{p,P,s}\right) l(T) + L_P D(T) & if\ T_s < T_P < T_l \\ C_{p,P,l} & if\ T_P \ge T_l \end{cases} \quad (9)$$

The balance of momentum in x direction for the PCM can be written in terms of density (ρ_P), velocity of PCM in x direction (u_x), velocity of PCM in y direction (u_y), pressure (p), dynamic viscosity (μ), gravitational force in x direction (g_x) and added body force (per unit volume) in x direction (F_x). First term on RHS is the pressure forces, second term on RHS is the viscous forces, third term on RHS is the buoyancy forces in x direction and fourth term on the RHS is the added body forces (per unit volume) in the x direction.

$$\rho_P \left(\frac{\partial u_x}{\partial t} + u_x \frac{\partial u_x}{\partial x} + u_y \frac{\partial u_x}{\partial y}\right) = -\frac{\partial p}{\partial x} + \mu \left(\frac{\partial^2 u_x}{\partial x^2} + \frac{\partial^2 u_x}{\partial y^2}\right) + \rho_P g_x - F_x \quad (10)$$

The balance of momentum in y direction for the PCM can be written in terms of density (ρ_P), velocity of PCM in x direction (u_x), velocity of PCM in y direction (u_y), pressure (p), dynamic viscosity (μ), gravitational force in y direction (g_y) and added body force (per unit volume) in y direction (F_y). First term on the RHS is the pressure forces, second term on RHS is the

viscous forces, third term on the RHS is the buoyancy forces in *y* direction and fourth term on the RHS is the added body forces (per unit volume) in the *y* direction.

$$\rho\left(\frac{\partial u_y}{\partial t}+u_x\frac{\partial u_y}{\partial x}+u_y\frac{\partial u_y}{\partial y}\right)=-\frac{\partial p}{\partial y}+\mu\left(\frac{\partial^2 u_y}{\partial x^2}+\frac{\partial^2 u_y}{\partial y^2}\right)+\rho g_y-F_y \quad (11)$$

The balance of mass for the PCM can be written in terms of the addition of the gradients of its velocities as follows,

$$\frac{\partial u_x}{\partial x}+\frac{\partial u_y}{\partial y}=0 \quad (12)$$

At the interface of phase change material and TCEC, the heat flow rate into the phase change material is same as that of the heat coming out from the aluminium. This equality can be written as follows,

$$k_P\frac{\partial T_P}{\partial y}=k_{al}\frac{\partial T_{al}}{\partial y}\ at\ interface\ perpendicular\ to\ y\ axis \quad (13)$$

$$k_P\frac{\partial T_P}{\partial x}=k_{al}\frac{\partial T_{al}}{\partial x}\ at\ interface\ perpendicular\ to\ x\ axis \quad (14)$$

At the interfaces of phase change material and containers, the velocity of PCM is 0 because of no-slip condition.

$$u_x=u_y=0\ at\ interface\ of\ PCM\ and\ aluminium \quad (15)$$

The charging efficiency is defined as the ratio of the rate of energy storage by PCM to the rate of heat generation in the system and the electrical efficiency of the PV is defined in terms of PV average temperature (T_{PV}) and solar irradiance on PV (I_T) as follows

$$\eta=0.2\left[1-0.005(T_{PV}-25)+0.085\ ln\left(\frac{I_T}{1000}\right)\right] \quad (16)$$

It must be mentioned that the grid independence study has been carried out to minimize the numerical modelling errors. Furthermore, in order to ensure the convergence of the solution, the time step has been chosen carefully. It must also be mentioned that in practical situations, it is difficult to make a perfect contact between PV rear and the PCM container. However, the current model considers perfect contact. By taking appropriate value for the contact resistance, the proposed model can be used to predict the effect of imperfect contact on the system's performance.

In the proposed model, a deterministic approach is used that takes fixed values for the input variables at a particular instant and gives a fixed value as output. However, by taking a range (instead of a single value) for any input variable by incorporating uncertainty, the model will produce a range as output (instead of a single value). In this way, the effect of uncertainty in the input parameters can be captured.

3. Experimental Validation

In order to verify the output of the equations, an experimental set up was manufactured by integrating a mono-si PV panel with eleven thermal conductivity enhancing containers and $CaCl_2$ $6H_2O$ as PCM as shown in Fig. 2 [37]. In Fig. 2a, the left one is the reference PV and the panel on the right side is the one with TCEC-PCM. Fig. 2b shows the back side of the PV-TCEC-PCM panel. The dimensions of PV panel are 1318 mm x 990 mm with a power rating of 175 Wp, electrical efficiency (at STC) of 13.5%, open circuit voltage of 29.8 V, short circuit current of 8.3 A, voltage corresponding to maximum power is 23.3 V and current corresponding to maximum power is 7.5 A. Eleven TCECs were manufactured using aluminium. The outer dimensions of each TCEC are 100 mm x 960 mm x 51 mm and the thickness of the material is 3 mm. The melting point of the PCM is around 30°C, the thermal conductivity is 1.08W/mK, the density is around 1710 kg/m^3, the latent heat capacity is 191 kJ/kg, the specific heat capacity is around 1400 J/kgK and the kinematic viscosity is 1.84 x 10^{-3} m^2/s. The PCM was filled inside the aluminium containers and the containers were pasted at back of the PV panel using heat sink paste. The clamps were used to tighten the contact of containers and the PV.

The experiments were run for a reference PV and PV-TCEC-PCM on 26th January at IIT Madras, Chennai, India. The measured values of solar irradiance, ambient temperature and average temperature of the front of the PV (for both systems) are displayed in Fig. 3. The computed values of the PV temperature are also plotted in Fig. 3. It can be seen that the computed results match well with the measured ones with a maximum difference of 3°C.

(a) (b)

Figure 2. (a) Reference PV panel and PV-TCEC-PCM panel; (b) Back side of the PV-TCEC-PCM panel [37]

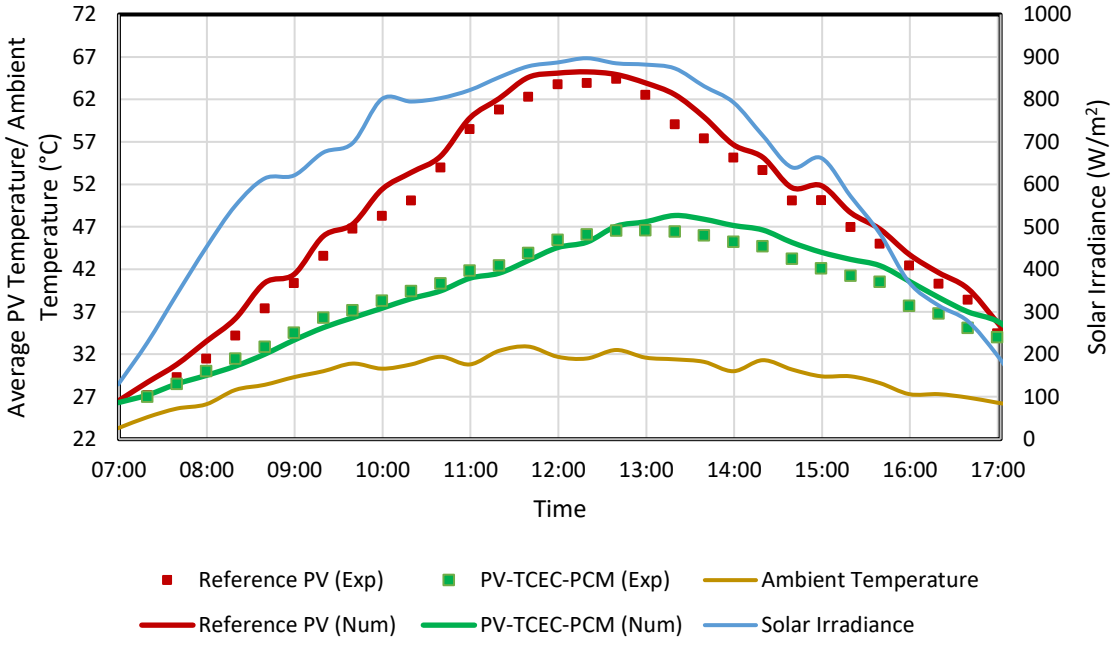

Figure 3. Solar irradiance, ambient temperature and average PV front temperature for reference PV and PV-TCEC-PCM panels

4. Results and Discussion and Comparison with Previous Studies

The transient analysis of all the seven systems has been carried out under the climatic conditions of Portsmouth, UK for the month of June. The weather data is presented in Appendix A. The melting process of PCM, charging efficiency, rate of energy storage and PV electrical efficiency are analyzed. The influence of inclination of the system and the use of TCEC are also investigated.

4.1. Melting Process of PCM

The transient analysis for the melting process of the PCM is shown in Fig. 4. The thermal images show that at 09:00h, most of the phase change material is in violet color which means that it is solid. At 11:00h, some of the PCM has changed its color from violet to light blue which means that it has changed its phase and reaches molten state. The thermal images also show that the solid PCM displaces the molten PCM and the solid PCM remains at bottom along the direction of gravity. The results presented by Huang et al. [9] have also shown the same type of phenomenon that the solid PCM displaces the molten PCM and solid PCM remains at bottom and liquid PCM at the top. At 13:00h, it can be seen that most of the PCM has changed its color to green which means that the molten PCM has raised its temperature. At 15:00h, the molten PCM has changed its color to orange which means that it is rising its temperature quickly. The results presented by Huang et al. [10] have also shown the same type of phenomenon that the molten PCM raises its temperature quickly due to the absorption of only sensible heat.

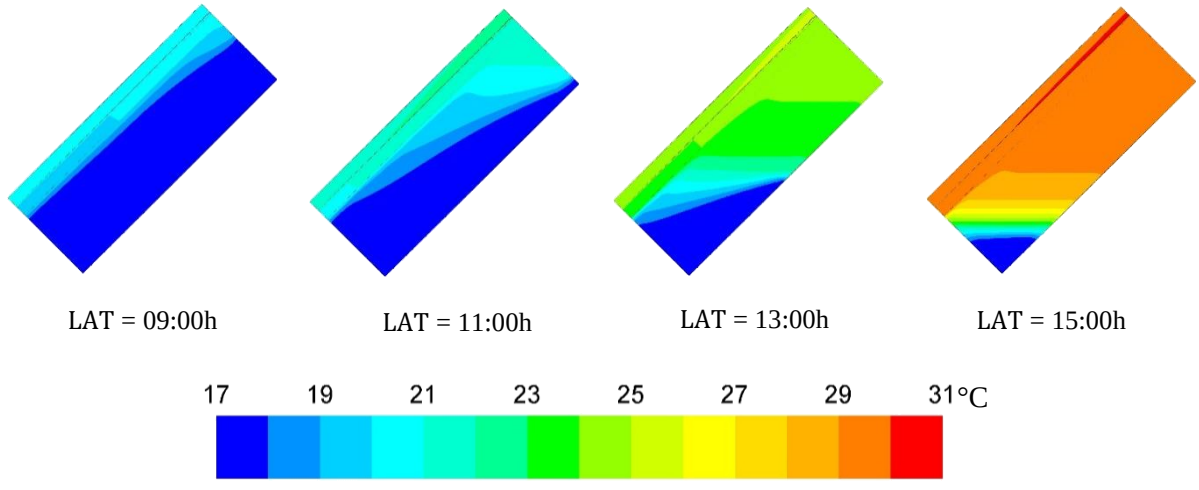

Figure 4. Thermal images of PV-PCM system.

4.2. Influence of Inclination Angle on Melting Process

In order to analyze the influence of inclination angle on the melting process of the PCM, various systems with different inclination angles are investigated. The transient analysis for the melting process of PCM in 4^{th}, 5^{th}, 6^{th} and 7^{th} systems is shown in Fig. 5. It can be seen that the system with 0° inclination angle (i.e. the horizontal system) raises its temperature quickly and at 13:00h-15:00h, a large amount of PCM is still in solid state denoted by violet color. On the other hand, the system with 45° inclination angle raises its temperature slowly and at 15:00h, a small amount of PCM is left in solid state. Thus, the increase in inclination angle raises the melting speed of the PCM due to increase in convective heat transfer. The results presented by Li et al. [38] have also shown the same phenomenon.

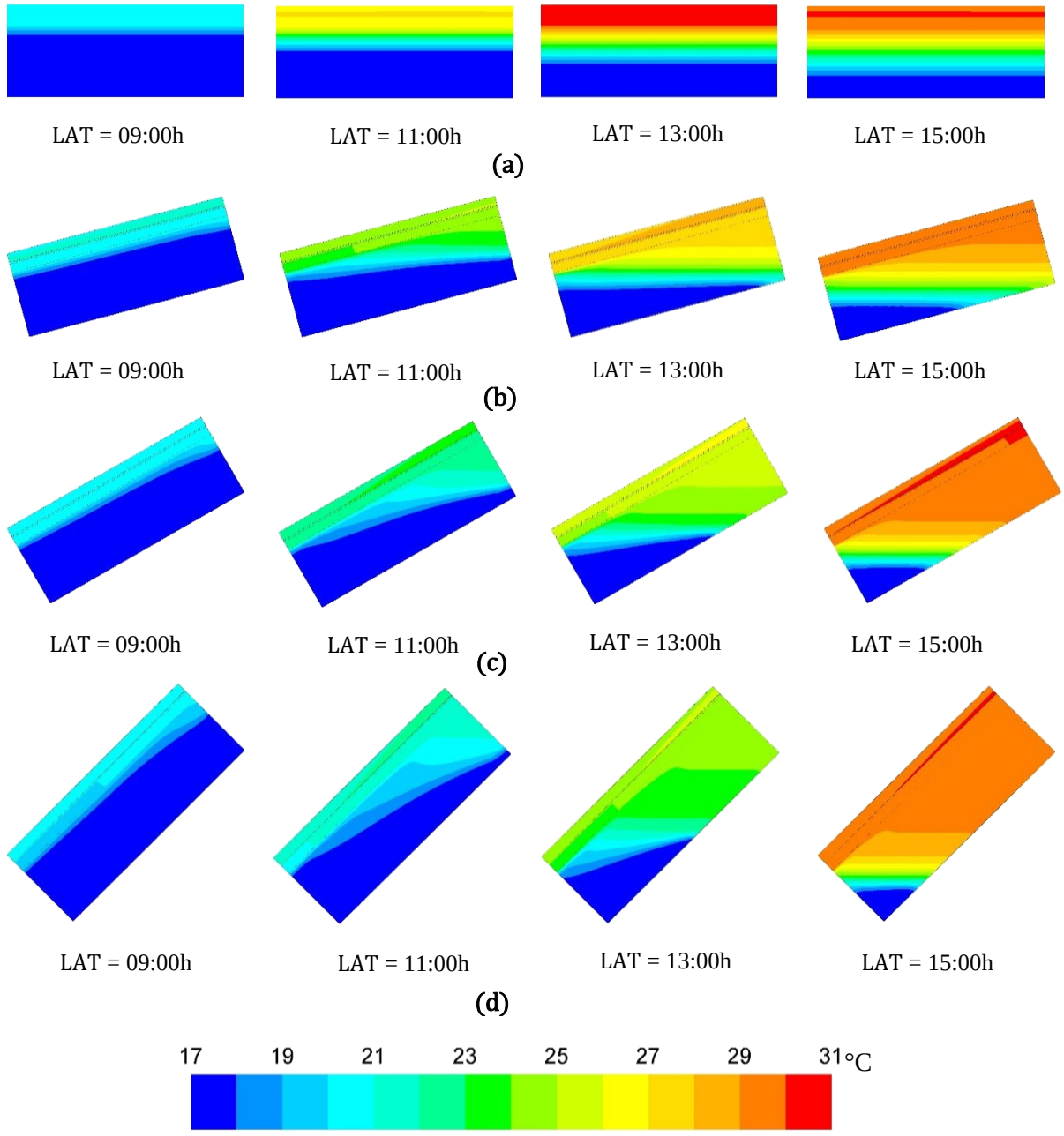

Figure 5. Thermal images of PVPCM systems (**a**) 4th system (0° inclination), (**b**) 5th system (15° inclination), (**c**) 6th system (30° inclination) and (**d**) 7th system (45° inclination).

4.3. Influence of TCEC on Melting Process of PCM

In order to analyze the influence of TCEC on the melting process of the PCM, PV-TCEC-PCM and PV-PCM systems are investigated. The thermal images for both systems are shown in Fig. 6. The images show that at 15:00h, the quantity of solid PCM is lesser in the case of PV-TCEC-PCM system as compared to PV-PCM system. Thus, it can be concluded that the use of TCECs increases the melting speed of PCM due to increase in conductive heat transfer. The thermal images also show that the temperature of PV decreases by using the TCECs. The results presented by Zarma et al. [26] have also shown that the thermal conductivity enhancement technique increases the rate of heat transfer and thus, increases the melting speed of PCM and reduces the PV temperature.

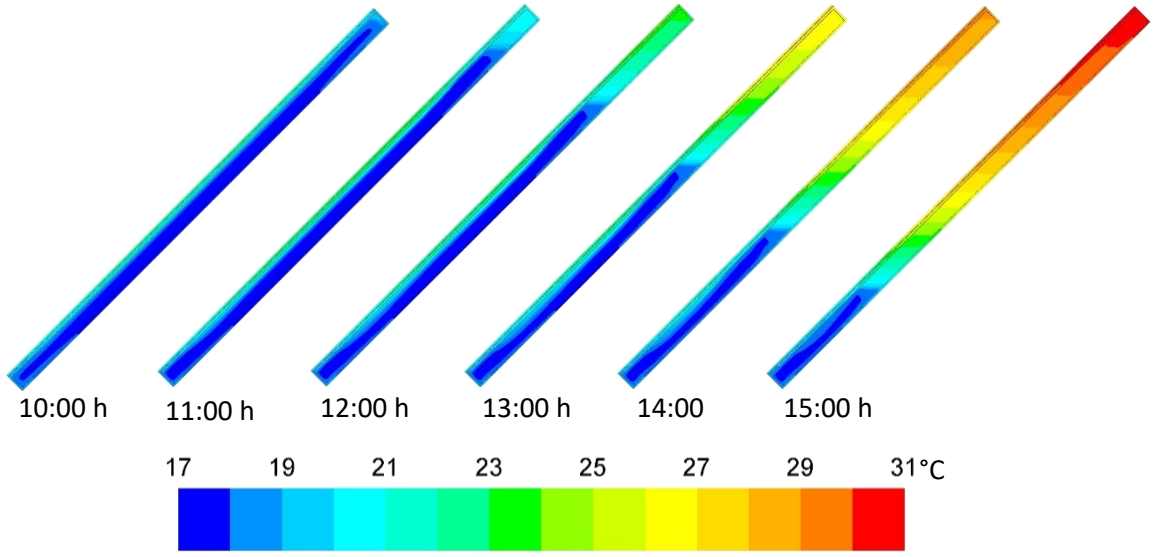

(**a**)

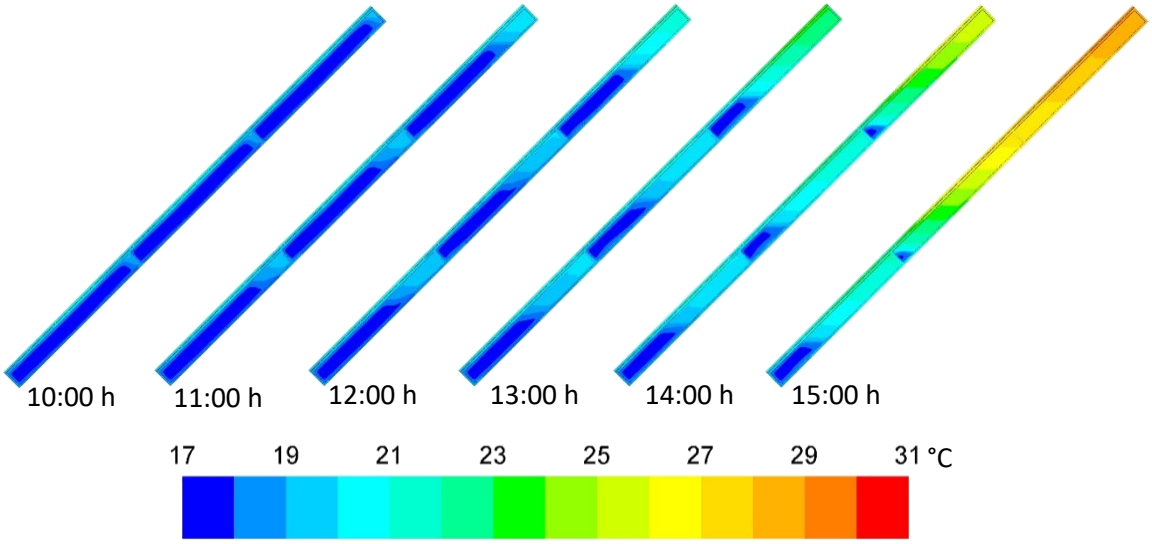

(**b**)

Figure 6. Thermal images of PV-PCM (2nd system) and PV-TCEC-PCM (3rd system).

4.4. Charging Efficiency of PCM

In order to analyze the charging efficiency of the PCM, the PV-PCM (2nd system) has been investigated. The change in the charging efficiency with time is shown in Fig. 7. It can be seen that, initially, the charging efficiency of the PCM is low since the PCM is in solid state. It is also because of low irradiance level. Later, the charging efficiency of PCM increases rapidly because the irradiance increases and the PCM is changing its phase and absorbing the heat in latent form. After 11:00h, the charging efficiency decreases with time since most of the PCM is completely liquefied. It can also be seen that the charging efficiency becomes negative near to the end of the day due to the fact that most of the PCM is in discharging mode.

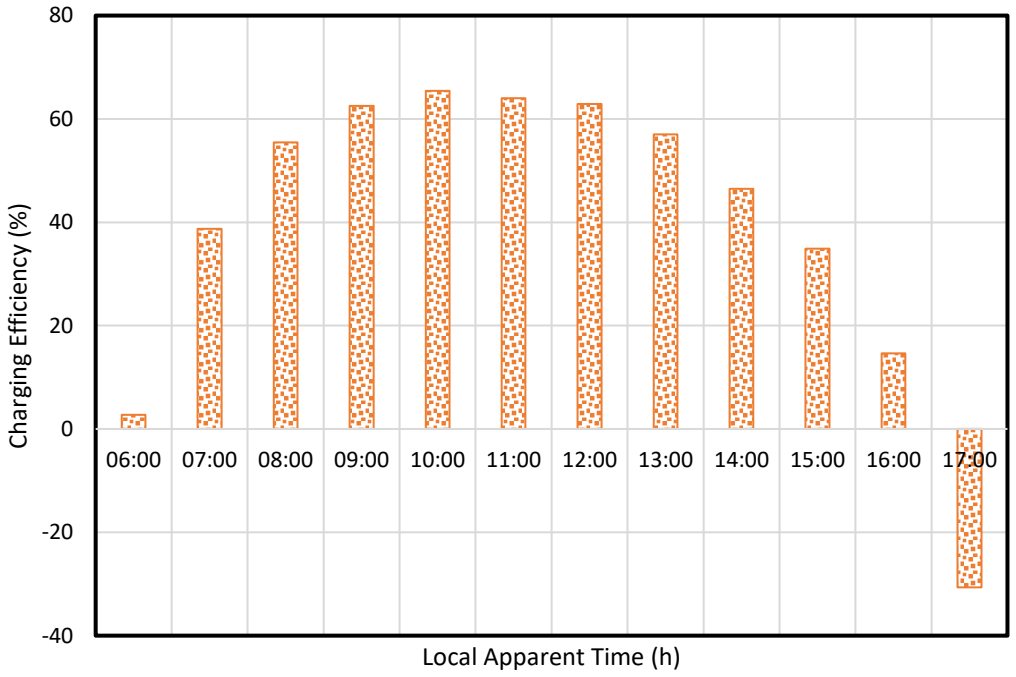

Figure 7. Charging efficiency of the PCM in PVPCM system (2nd system).

4.5. Influence of TCEC on the Charging Efficiency of PCM system

In order to analyze the influence of TCEC on the charging efficiency, PV-PCM and PV-TCEC-PCM systems are investigated. The changes in the charging efficiency of the PCM with time are shown in Fig. 8 and the average charging efficiency is plotted in Fig. 9. It can be seen that the TCECs increase the average charging efficiency of the PCM from 49% to 62% over the charging period (Fig. 9). It is due to the fact that the heat flows from PV to TCEC. Due to high thermal conductivity of TCEC material, all the sides of the TCEC get heated up and the PCM starts absorbing heat from all sides which increases the conductive heat transfer. Thus, the use of TCEC increases the charging efficiency. After noon, it can be seen that the charging efficiency of PV-TCEC-PCM system is much higher as compared to PV-PCM system (Fig. 8) since the PCM is liquefied unevenly in PV-PCM system which means that some of the PCM is completely solid and some of the PCM is completely liquid. On the other hand, in PV-TCEC-PCM system, the PCM is liquefied evenly. The results presented by Zarma et al. [26] have also shown the same type of phenomenon that the use of thermal conductivity enhancement technique increases the uniformity of the PCM melting, increases the rate of heat transfer and thus, increases the efficiency.

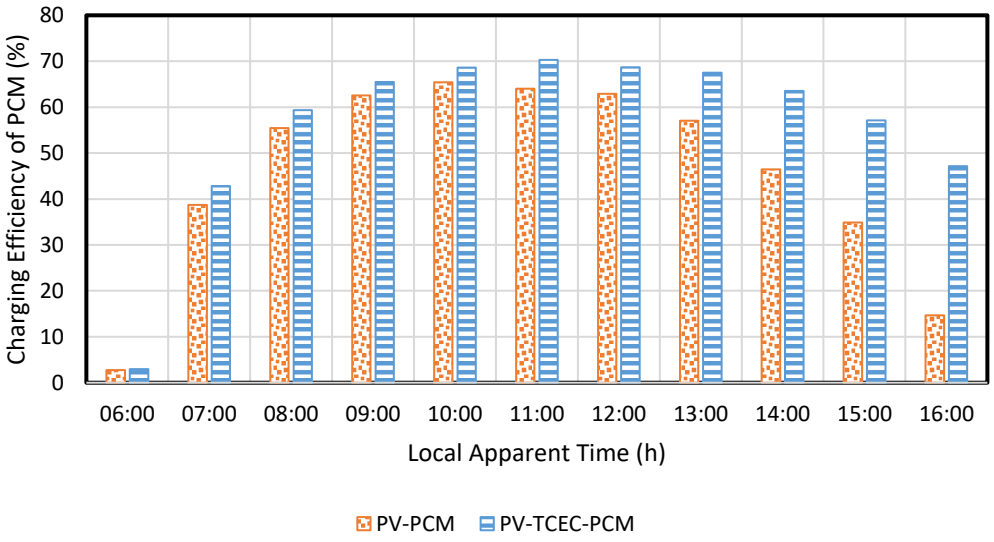

Figure 8. Charging efficiency of the PCM.

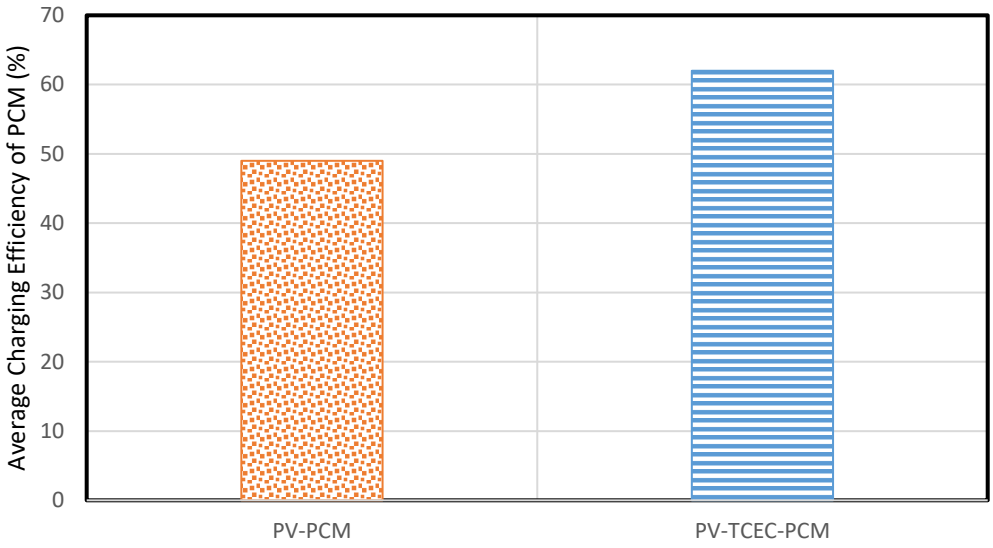

Figure 9. Average charging efficiency of the PCM during the charging period.

4.6. Influence of Inclination on the Charging Efficiency of PCM system

In order to analyze the influence of inclination angle on the charging efficiency, systems with different inclination angles are investigated. The average charging efficiency of PCM in PV-PCM systems is shown in Fig. 10. It can be seen that the system with 0° inclination angle, which is horizontal, achieves a charging efficiency of 33%. The average charging efficiency of the system with 45° inclination is 49%. Thus, the increase in inclination increases the charging efficiency. It is due to the fact that, for horizontal system, the heat transfer in the PCM takes place mostly due to conduction. On the other hand, the inclination of the system increases the heat transfer due to convection which increases the charging efficiency of the PCM.

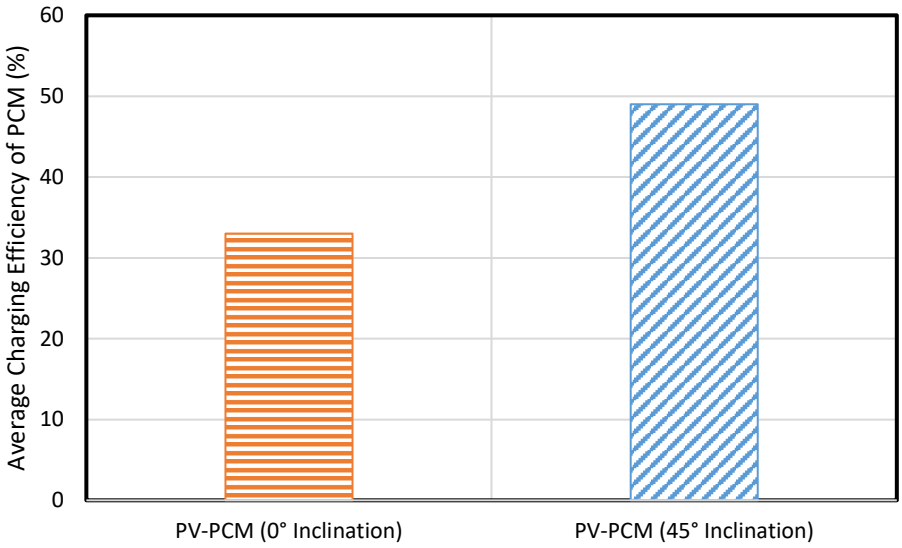

Figure 10. Average charging efficiency of the PCM with different inclination angles during the charging period.

4.7. Rate of Thermal Energy Storage

In order to analyze the rate of energy storage, the PVPCM systems are analyzed. The change in the rate of energy storage along the day is shown in Fig. 11. It can be seen that, early morning, the rate of energy storage is low because the PCM is in solid state and it is absorbing energy as sensible heat. It is also because of low irradiance level. Later, the rate of energy storage increases because the irradiance increases and the PCM is changing its phase and absorbing the heat in latent form. After 11:00h, the energy storage rate decreases with time since most of the PCM is completely liquefied. It can also be seen that the rate of energy storage becomes negative near to the end of the day as most of the PCM is in discharging mode at that time.

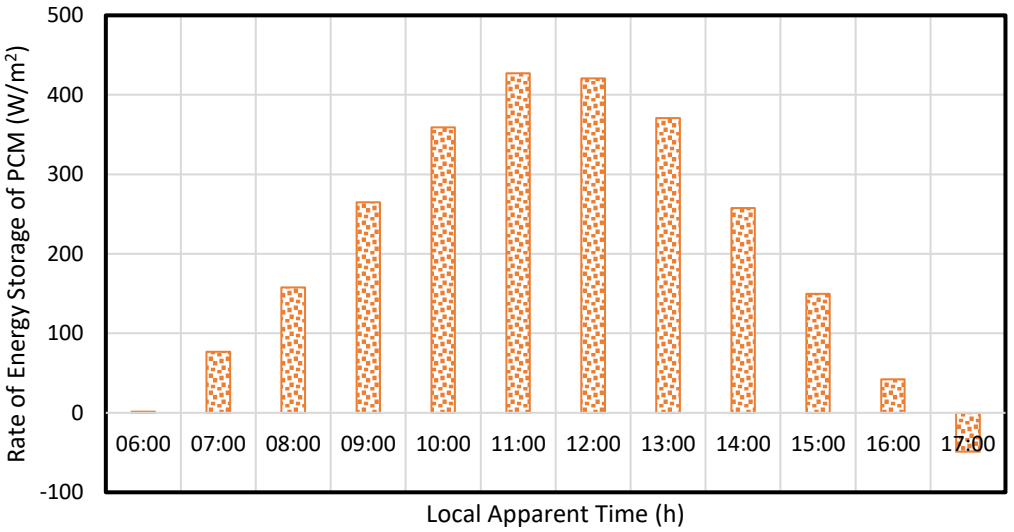

Figure 11. Rate of thermal energy storage of the PCM in PCM systems.

4.8. Influence of TCEC on the Rate of Energy Storage

In order to analyze the influence of TCEC on the rate of energy storage, PV-PCM and PV-TCEC-PCM systems are investigated. The changes in the rate of energy storage along the day are shown in Fig. 12 and the average rate of energy storage is shown in Fig. 13. It can be seen that the TCEC increases the average rate of energy storage of the PCM from 249 to 302 W/m^2 during the charging period (Fig. 13). It is because of an increase in the contact surface of the PCM with aluminium which increases the conductive heat transfer. After noon, it can be seen that the rate of energy storage in PV-TCEC-PCM system is much higher as compared to PV-PCM system (Fig. 13). It is because of the uneven melting of the PCM in PV-PCM system. On the other hand, in PV-TCEC-PCM system, PCM is melted evenly.

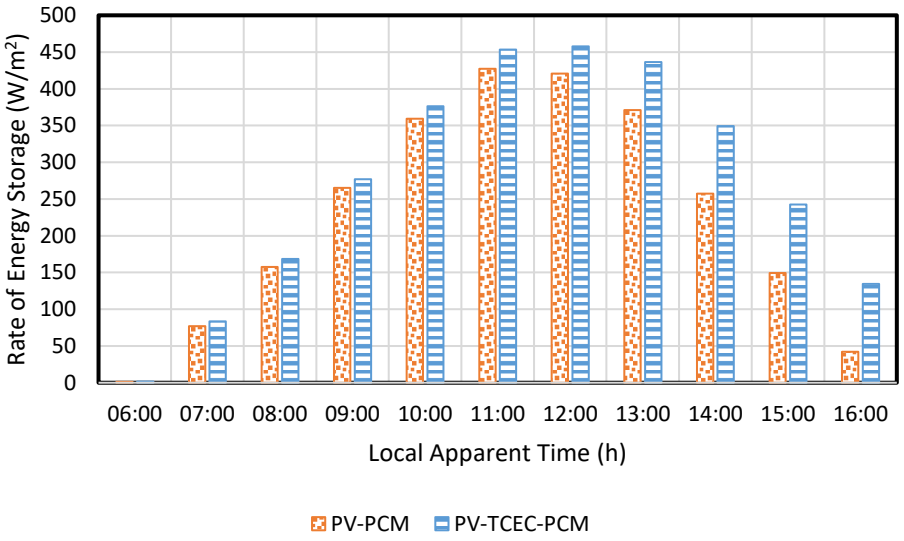

Figure 12. Rate of thermal energy storage by the PCM.

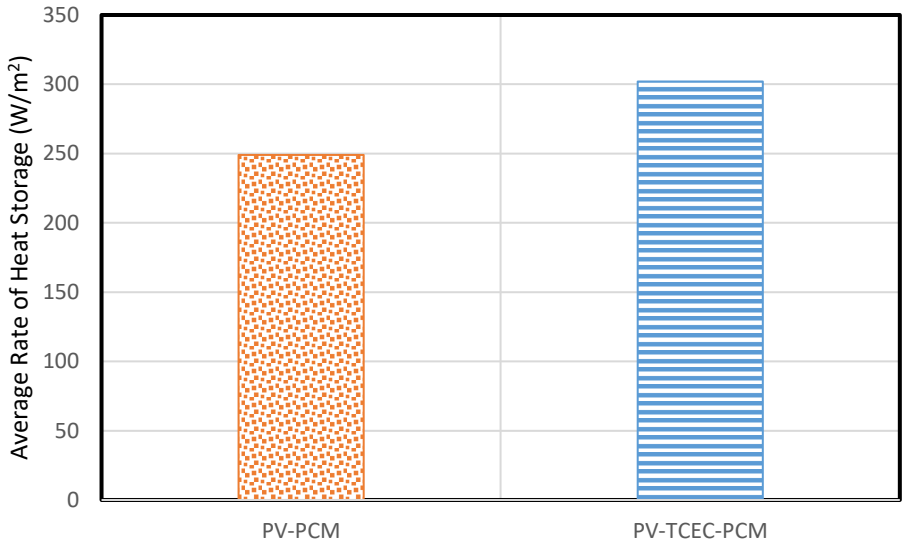

Figure 13. Average rate of thermal energy storage by the PCM during the charging period.

4.9. Influence of Inclination on the Rate of Energy Storage

In order to analyze the influence of inclination angle on the rate of energy storage, systems with different inclination angles are investigated. The average rate of energy storage in PV-PCM systems is shown in Fig. 14. It can be seen that the system with 45° inclination angle achieves a rate of energy storage of 249 W/m^2. On the other hand, the system with 0° inclination (horizontal system) can achieve a rate of energy storage of just 180 W/m^2. Thus, the decrease in inclination decreases the rate of energy storage significantly. It is due to the fact that for horizontal system, the heat transfer in the PCM due to convection becomes negligible which decreases the rate of energy storage.

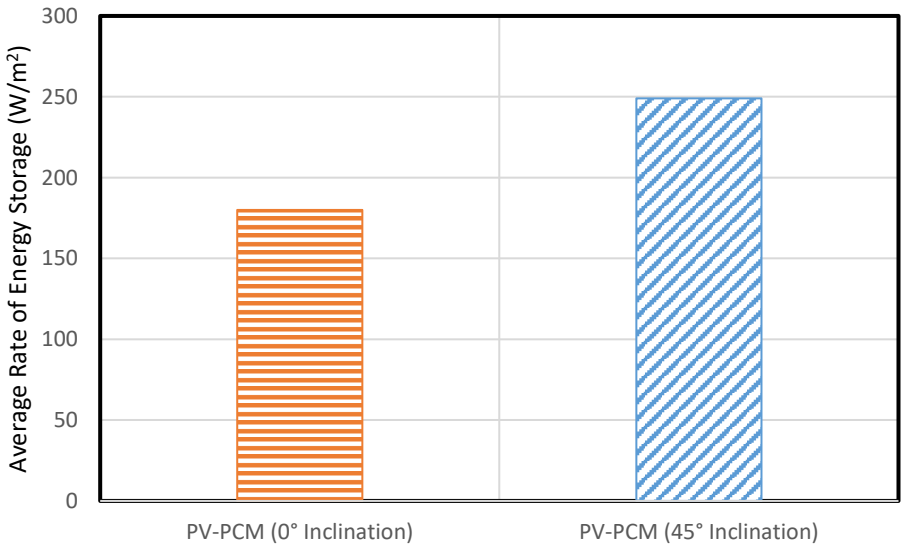

Figure 14. Average rate of energy storage during the charging period.

4.10. Electrical Efficiency

In order to analyze the effectiveness of PV-PCM and PV-TCEC-PCM systems, the electrical efficiency of PV panels for different systems are compared with that of reference PV. The power production efficiency of all the systems is plotted in Fig. 15. It can be seen that, around noon, the PV efficiency of reference panel is 17.6%. Using PCM, the PV efficiency increases to 18.9%. Using the TCEC-PCM system, it increases to 19.2%. The reason behind the increase in the PV efficiency is the increase in the open circuit voltage by the cooling of PV which was explained by Sharma et al. [27] too.

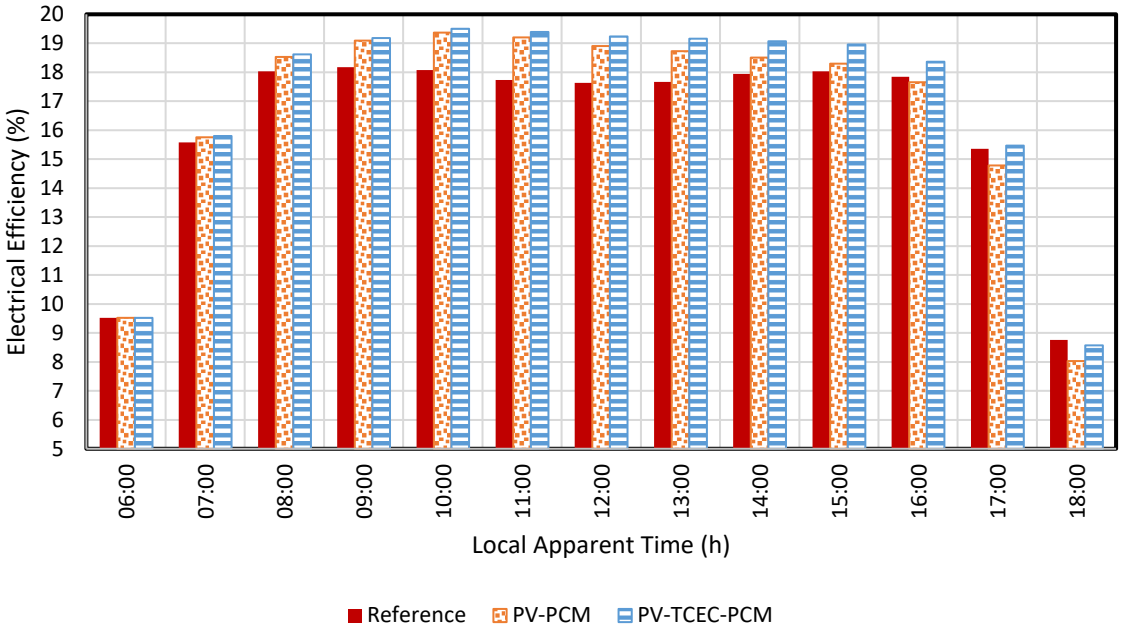

Figure 15. Efficiency of PV in different systems.

5. Conclusions

The present work aims at improvement in the charging efficiency of PCM and improvement in the PV performance by using thermal conductivity enhancing containers (TCEC). Systems with and without PCM, with and without TCECs and systems with different tilt angles have been investigated. The transient analysis has been carried out experimentally and numerically for the climatic conditions of Chennai, India. For Portsmouth (UK), the analysis has been carried out numerically. It has been found that

(i) The power production efficiency of PV can be increased from 17.6% to 19.2% using proposed TCEC-PCM.

(ii) The average charging efficiency of PCM can be increased by 13% using the TCECs.

(iii) The decrease in the inclination from 45° to 0° can decrease the average charging efficiency of PCM to 33%.

(iv) The average rate of thermal energy storage in PVPCM system is 249 W per m^2 of aperture area and it increases to 302 W per m^2 by using TCEC.

(v) The decrease in the inclination from 45° to 0° can decrease the average rate of thermal energy storage from 249 W/m^2 to 180 W/m^2.

It must be mentioned that the PCM is expensive and the additional investment in the form of PCM can be higher than that of the savings in certain cases. However, mass production of PCM can bring the cost down and, thus, PCM integration with PV can become cost effective. As mentioned earlier, it must also be noted that some type of PCMs do not solidify homogenously affecting the contact of solid PCM with the walls of the containers which was not considered in the mathematical model. It must be incorporated in the future studies. The imperfect contact of the PV rear with the PCM container must also be incorporated using contact resistances while modeling. It must be mentioned that the analysis of the full discharging period (i.e. over the night) has not been shown in the present study which is

required to analyze whether the PCM is able to solidify properly or not for the next day. On the other hand, Hasan et al. [17] have shown the results for the night hours too. It must also be mentioned that the present study evaluates the performance of the proposed system for a sunny day. However, annual performance analysis should be carried out to evaluate how much performance enhancement can be achieved annually. For example: Kazemian et al. [39] and Hasan et al. [40] have carried out annual studies for their systems.

Appendix A

Table A.1 Specifications

Parameter	Value
$C_{p,al}$	0.9 kJ kg^{-1} K^{-1}
$C_{p,EVA}$	2.1 kJ kg^{-1} K^{-1}
$C_{p,gl}$	0.5 kJ kg^{-1} K^{-1}
$C_{p,P,l}$	2.0 kJ kg^{-1} K^{-1}
$C_{p,P,s}$	2.0 kJ kg^{-1} K^{-1}
$C_{p,si}$	0.7 kJ kg^{-1} K^{-1}
$C_{p,t}$	1.3 kJ kg^{-1} K^{-1}
L_p	260 kJ kg^{-1}
k_{al}	211 W m^{-1} K^{-1}
k_{EVA}	0.35 W m^{-1} K^{-1}
k_{gl}	1.8 W m^{-1} K^{-1}
$k_{P,l}$	0.2 W m^{-1} K^{-1}
$k_{P,s}$	0.2 W m^{-1} K^{-1}
k_{si}	148 W m^{-1} K^{-1}
k_t	0.2 W m^{-1} K^{-1}
L	25cm
$T_{P,s}$	290 K
$T_{P,l}$	292 K
t_{al}	4 mm
t_{EVA}	0.5 mm
t_{gl}	3 mm
t_{si}	0.3 mm
t_t	0.1 mm
ε	0.85
μ_l	0.0018 kg m^{-1} s^{-1}
ρ_{al}	2675 kg m^{-3}
ρ_{EVA}	960 kg m^{-3}
ρ_{gl}	3000 kg m^{-3}
$\rho_{P,l}$	770 kg m^{-3}
$\rho_{P,s}$	880 kg m^{-3}
ρ_{si}	2330 kg m^{-3}
ρ_t	1200 kg m^{-3}

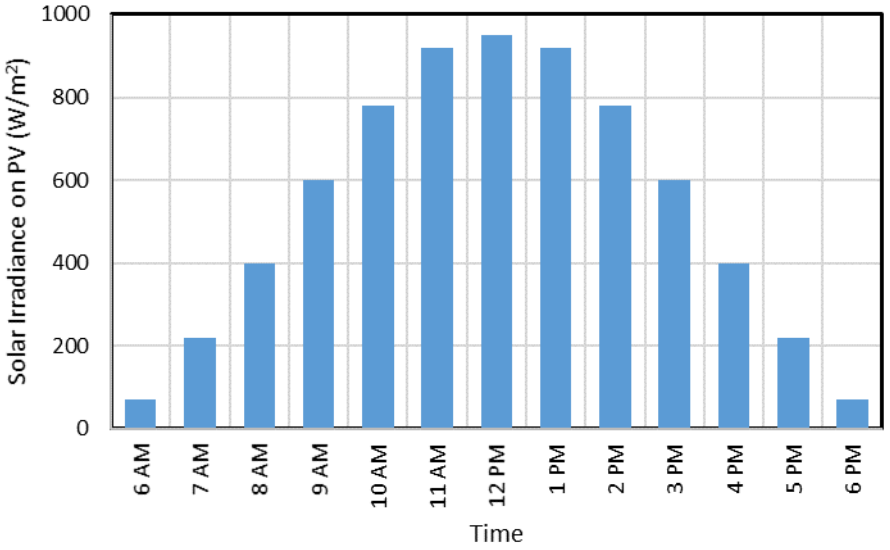

(**a**)

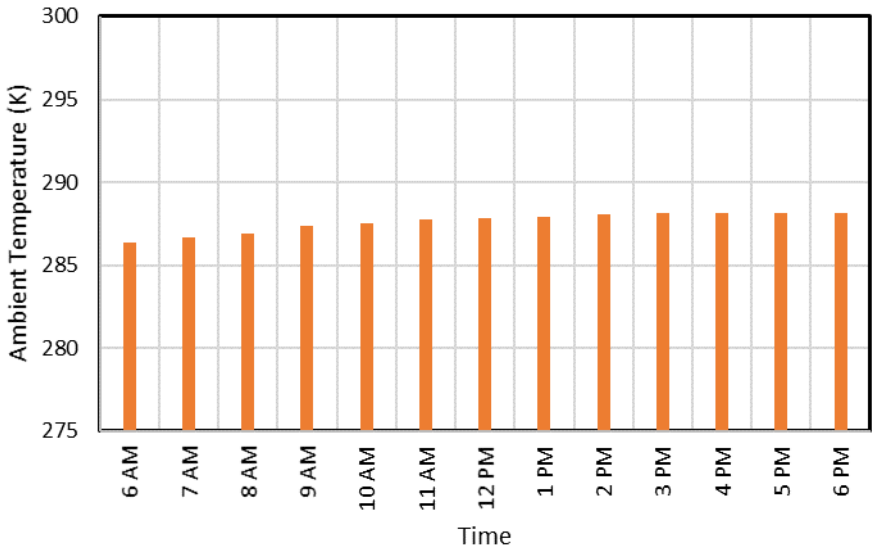

(**b**)

Figure A1. Weather data

References

1. Ahmad et al., 2020. Recent advances and applications of solar photovoltaics and thermal technologies. Energy 207, 118254. https://doi.org/10.1016/j.energy.2020.118254
2. Al Siyabi I., Khanna S., Sundaram S., Mallick T., 2019. Experimental and numerical thermal analysis of multi-layered microchannel heat sink for concentrating photovoltaic application. Energies 12(1) 122. https://doi.org/10.3390/en12010122
3. Nizetic et al., 2021. Implementation of phase change materials for thermal regulation of photovoltaic thermal systems: Comprehensive analysis of design approaches. Energy 120546. https://doi.org/10.1016/j.energy.2021.120546
4. Barone et al., 2020. Passive and active performance assessment of building integrated hybrid solar photovoltaic/thermal collector prototypes: Energy, comfort, and economic analyses. Energy 209, 118435.
5. Atkin and Farid, 2015. Improving the efficiency of photovoltaic cells using PCM infused graphite and aluminium fins. Solar Energy 114, 217–228.
6. M. C. Pournami, B. Sreenath and R. Zachariah, "A comprehensive review on the recent advancements in PV panel cooling techniques using phase changing materials," 2017 IEEE International Conference on Intelligent Techniques in Control, Optimization and Signal Processing (INCOS), 2017, pp. 1-6, doi: 10.1109/ITCOSP.2017.8303153.
7. D. Weber et al., "Lifetime Extension of Photovoltaic Modules by Influencing the Module Temperature Using Phase Change Material," 2018 IEEE 7th World Conference on Photovoltaic Energy Conversion (WCPEC), pp. 0784-0789, doi: 10.1109/PVSC.2018.8548115.
8. I. Das Chowdhury, S. Ghosal, S. Roy and K. Sengupta, "Utilization of Phase Change Material for Raising Conversion Efficiency of PV Cell: A Review," 2020 IEEE 1st International Conference for Convergence in Engineering (ICCE), 2020, pp. 54-59, doi: 10.1109/ICCE50343.2020.9290663.

9. Huang et al., 2006. Phase change materials for limiting temperature rise in building integrated photovoltaics. Solar Energy 80, 1121–1130.
10. Huang et al., 2006. Comparison of a small-scale 3D PCM thermal control model with a validated 2D PCM thermal control model. Solar Energy Materials & Solar Cells 90, 1961–1972.
11. Khanna S., Newar S., Sharma V., Reddy K.S., Mallick T.K., Radulovic J., Khusainov R., Hutchinson D., Becerra V., 2019. Electrical enhancement period of solar photovoltaic using phase change material. Journal of Cleaner Production 221, 878-884. https://doi.org/10.1016/j.jclepro.2019.02.169
12. Elarga et al., 2016. Thermal and electrical performance of an integrated PV-PCM system in double skin façades: A numerical study. Solar Energy 136, 112–124. https://doi.org/10.1016/j.solener.2016.06.074
13. Singh P., Khanna S., Becerra V., Newar S., Sharma V., Mallick T.K., Hutchinson D., Radulovic J., Khusainov R., 2020. Power improvement of finned solar photovoltaic phase change material system. Energy 193, 116735. https://doi.org/10.1016/j.energy.2019.116735
14. Khanna S., Reddy K.S., Mallick T.K., 2018. Effect of climate on electrical performance of finned phase change material integrated solar photovoltaic. Solar Energy 174, 593–605. https://doi.org/10.1016/j.solener.2018.09.023
15. J. Sarwar, A. E. Abbas and K. E. Kakosimos, "Effect of the thermophysical properties of a phase change material on the electrical output of a concentrated photovoltaic system," 2017 IEEE 44th Photovoltaic Specialist Conference (PVSC), 2017, pp. 1888-1892, doi: 10.1109/PVSC.2017.8366646.
16. Waqas et al., 2018. Thermal and electrical management of photovoltaic panels using phase change materials – A review. Renewable and Sustainable Energy Reviews 92, 254–271.

17. Hasan et al., 2015. Increased photovoltaic performance through temperature regulation by phase change materials: Materials comparison in different climates. Solar Energy 115, 264-276.
18. Karthick et al., 2018. Performance enhancement of a building-integrated photovoltaic module using phase change material. Energy 142, 803-812.
19. Karthick et al. 2020. Investigation of a binary eutectic mixture of phase change material for building integrated photovoltaic (BIPV) system. Solar Energy Materials and Solar Cells 207, 110360
20. Thaib et al., 2018. Experimental analysis of using beeswax as phase change materials for limiting temperature rise in building integrated photovoltaics. Case Studies in Thermal Engineering 12, 223-227.
21. Abdollahi and Rahimi, 2020. Potential of water natural circulation coupled with nano-enhanced PCM for PV module cooling. Renewable Energy 147, 302-309.
22. E. Japs, S. Peters, G. Sonnenrein and S. Krauter, 2014. Energy-economic comparison of photovoltaic modules equipped with a layer of conventional and improved phase-change material. IEEE 40th Photovoltaic Specialist Conference (PVSC), pp. 1348-1352, doi: 10.1109/PVSC.2014.6925167.
23. F. Kawtharani et al., 2017. Cooling PV modules using phase change material. IEEE 29th International Conference on Microelectronics (ICM), pp. 1-5, doi: 10.1109/ICM.2017.8268830.
24. Jamil et al., 2021. Evaluation of photovoltaic panels using different nano phase change material and a concise comparison: An experimental study. Renewable Energy 169, 1265-1279.
25. Al-Waeli et al., 2019. Experimental investigation of using nano-PCM/nanofluid on a photovoltaic thermal system (PVT): Technical and economic study. Thermal Science and Engineering Progress 11, 213-230.

26. Zarma et al., 2019. Enhancing the performance of concentrator photovoltaic systems using Nanoparticle-phase change material heat sinks. Energy Conversion and Management 179, 229–242.
27. Sharma et al., 2017. Nano-enhanced Phase Change Material for thermal management of BICPV. Appl Energy 208, 719–33.
28. Manigandan and Kumar, 2019. Comparative study to use nanofluid ZnO and CuO with phase change material in photovoltaic thermal system. International Journal of Energy Research 43(5), 1882-1891. https://doi.org/10.1002/er.4442
29. Salem et al., 2019. Performance enhancement of the photovoltaic cells using Al2O3 /PCM mixture and/or water cooling-techniques. Renewable Energy 138, 876–90.
30. Nada and El-Nagar, 2018. Possibility of using PCMs in temperature control and performance enhancements of free stand and building integrated PV modules. Renewable Energy 127, 630–41.
31. Luo et al., 2017. Numerical and experimental study on temperature control of solar panels with form-stable paraffin/expanded graphite composite PCM. Energy Conversion and Management 149, 416–423.
32. Khanna S., Newar S., Sharma V., Reddy K.S., Mallick T.K. 2019. Optimization of fins fitted phase change material equipped solar photovoltaic under various working circumstances. Energy Conversion and Management 180, 1185-1195. https://doi.org/10.1016/j.enconman.2018.10.105
33. Shastry and Arunachala, 2020. Thermal management of photovoltaic module with metal matrix embedded PCM. Journal of Energy Storage 28, 101312. https://doi.org/10.1016/j.est.2020.101312
34. Abdelrahman et al., 2019. Performance enhancement of photovoltaic cells by changing configuration and using PCM (RT35HC) with nanoparticles Al2O3. Solar Energy 177, 665–71.

35. Wongwuttanasatian et al., 2020. Performance enhancement of a photovoltaic module by passive cooling using phase change material in a finned container heat sink. Solar Energy 195, 47–53.
36. Biwole et al., 2013. Phase-change materials to improve solar panel's performance. Energy and Buildings 62, 59-67.
37. Singh P., Mudgal V., Khanna S., Mallick T.K., Reddy K.S. 2020. Experimental investigation of solar photovoltaic panel integrated with phase change material and multiple conductivity-enhancing-containers. Energy 205, 118047. https://doi.org/10.1016/j.energy.2020.118047
38. Li et al., 2021. Experimental and numerical study on performance enhancement of photovoltaic panel by controlling temperature with phase change material. International Journal of Energy Research 45, 16062–16077. https://doi.org/10.1002/er.6836
39. Kazemian et al., 2020. A year-round study of a photovoltaic thermal system integrated with phase change material in Shanghai using transient model. Energy Conversion Management 210, 112657. https://doi.org/10.1016/j.enconman.2020.112657
40. Hasan et al., 2017. Yearly energy performance of a photovoltaic-phase change material (PV-PCM) system in hot climate. Solar Energy 146, 417-429. http://dx.doi.org/10.1016/j.solener.2017.01.070.